

Analysis on Signal-in-Space Range Error and Positioning Accuracy of BDS-3

Weiping Liu (✉ lwpchxy@sina.com)

Information Engineering University

Bo Jiao

Information Engineering University

Jinming Hao

Information Engineering University

Zhiwei Lv

Information Engineering University

Jiantao Xie

Information Engineering University

Jing Liu

Information Engineering University

Research Article

Keywords: BDS-3, Signal-in-space range error, Standard point positioning, Precise point positioning, Different code bias

Posted Date: December 16th, 2021

DOI: <https://doi.org/10.21203/rs.3.rs-1048713/v1>

License:  This work is licensed under a Creative Commons Attribution 4.0 International License.

[Read Full License](#)

1

2 **Analysis on Signal-in-Space Range Error and Positioning Accuracy of BDS-3**

3 Weiping Liu, Bo Jiao, Jinming Hao, Zhiwei Lv, Jiantao Xie, Jing Liu

4 Information Engineering University, Zhengzhou 450001, China

5 ***Corresponding to:** Weiping Liu

6 **Email:** lwpchxy@163.com

7

8 **Abstract** Being the first mixed-constellation global navigation system, the global BeiDou
9 navigation system (BDS-3) designs new signals, the service performance of which has
10 attracted extensive attention. In the present study, the Signal-in-space range error (SISRE)
11 computation method for different types of navigation satellites was presented. And the
12 differential code bias (DCB) correction method for BDS-3 new signals was deduced. Based
13 on these, analysis and evaluation were done by adopting the actual measured data after the
14 official launching of BDS-3. The results showed that BDS-3 performed better than the
15 regional navigation satellite system (BDS-2) in terms of SISRE. Specifically, the SISRE of
16 the BDS-3 medium earth orbit (MEO) satellites reached 0.52 m, slightly inferior compared to
17 0.4 m from Galileo, marginally better than 0.57 m from GPS, and significantly better than
18 2.33 m from GLONASS. And the BDS-3 inclined geostationary orbit (IGSO) satellites
19 achieved the SISRE of 0.90 m, on par with that of the QZSS IGSO satellites. However, the
20 average SISRE of BDS-3 geostationary earth orbit (GEO) satellites was 1.15 m, which was
21 marginally inferior to that of the QZSS GEO satellite (0.91m). In terms of positioning
22 accuracy, the overall three-dimensional single-frequency standard point positioning (SPP)
23 accuracy of BDS-3 B1C, B2a, B1I, and B3I gained an accuracy level better than 5 m.
24 Moreover, the B1I signal exhibited the best positioning accuracy in the Asian-Pacific region,
25 while the B1C signal set forth the best positioning accuracy in the other regions. Owing to the
26 advantage in signal frequency, the dual-frequency SPP accuracy of B1C+B2a surpassed that
27 of the transitional signal of B1I+B3I. Since there are more visible satellites in Asia-Pacific,
28 the positioning accuracy of BDS-3 was moderately superior to that of GPS. The precise point
29 positioning (PPP) accuracy of BDS-3 B1C+B2a or B1I+B3I converged to the order of
30 centimeters, marginally inferior to that of the GPS L1+L2. However, these three combinations

31 had a similar convergence time of approximately 30 minutes.

32

33 **Keywords:** BDS-3; Signal-in-space range error; Standard point positioning; Precise point
34 positioning; Different code bias

35

36 **Introduction**

37 According to a steady “three-step” strategy^[1], BeiDou Navigation Satellite System (BDS)
38 is independently established and operated by China. On July 31st, 2020, based on the
39 demonstration navigation satellite system (BDS-1) and the regional navigation satellite
40 system (BDS-2), the global BeiDou navigation system (BDS-3) was officially announced as
41 operational. BDS-3 comprises 3 geostationary earth orbit (GEO) satellites, 3 inclined
42 geostationary orbit (IGSO) satellites, and 24 medium earth orbit (MEO) satellites^[2]**Error!**
43 **Reference source not found.** All these satellites have been providing services normally except for the
44 last launched GEO satellite. Considering that BDS-2 still has 5 GEO satellites, 7 IGSO
45 satellites, and 3 MEO satellites that are functioning normally in orbit, the current BeiDou
46 System has a total of 44 operational satellites in orbit that can provide services. The
47 corresponding satellite types are listed in Table 1. The tracks of sub-satellite points are
48 illustrated in Figure 1, in which the red line represents the BDS-2 satellites while the blue
49 indicates the BDS-3 satellites. BDS-3 adopts the new signals B1C (1575.42MHz) and B2a
50 (1176.45MHz) for open service, which are broadcast on the BDS-3 MEO and IGSO
51 satellites^{[3][4][5]}. Concurrently, for smooth transitioning with BDS-2, all types of BDS-3
52 satellites allow for compatible broadcasting of B1I (1561.098MHz) and B3I
53 (1207.14MHz)^{[6][7]}, as mentioned in Table 2. A series of improvements have been inculcated
54 in the ground segment of BDS-3^[8], and the inter-satellite link is added at its space segment^[9].
55 The performance of the ground segment and the space segment demands in-depth analysis
56 and evaluation. Besides, the positioning performance of the new signals and the transitional
57 signals is a matter of concern for the user segment.

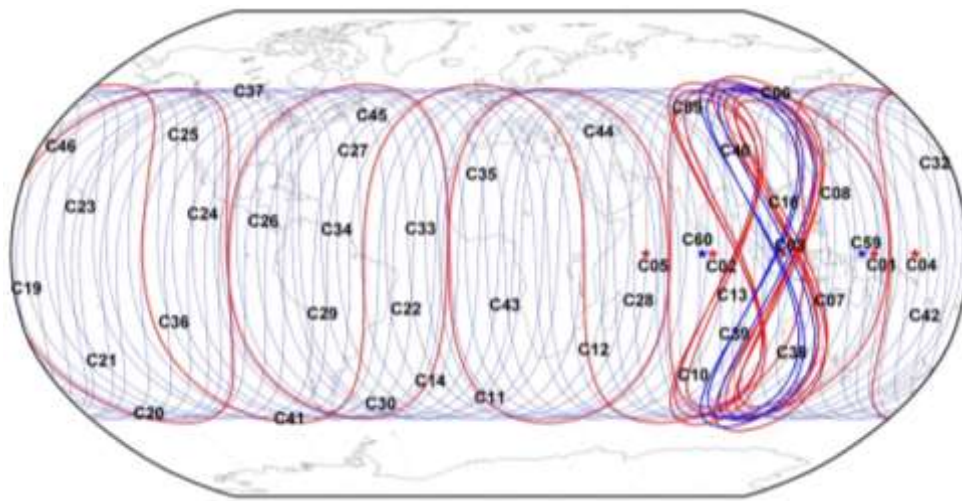
58

59 **Table 1** Operational BeiDou System satellites in orbit. The last launched BDS-3 GEO
60 satellite C61 isn’t included, because it is still in the in-orbit testing phase when the paper is

61 completed.

System	Satellite type	PRN
	GEO	C01-C05
BDS-2	IGSO	C06-C10, C13, C16
	MEO	C11, C12, C14
	GEO	C59, C60
BDS-3	IGSO	C38-C40
	MEO	C19-C30, C32-C37, C41-C46

62



63

64 **Fig. 1** Tracks of sub-satellite points for in-orbit operational BeiDou satellites. The red and
 65 blue lines denote BDS-2 and BDS-3 satellites, respectively.

66

67 **Table 2** Open service signals of BeiDou System. B1C and B2a are the new signals of BDS-3,
 68 while B1I and B3I are the compatible signals of both BDS-2 and BDS-3.

Signal	Center frequency (MHz)	Broadcasting satellites
B1C	1575.42	BDS-3: 3IGSO+24MEO
B2a	1176.45	BDS-3: 3IGSO+24MEO
B1I	1561.098	BDS-2: 5GEO+7IGSO+3MEO
		BDS-3: 3GEO+3IGSO+24MEO
B3I	1268.52	BDS-2: 5GEO+7IGSO+3MEO
		BDS-3: 3GEO+3IGSO+24MEO

69

70 The Signal-in-space range error (SISRE) reflects the error of the broadcast ephemeris
71 orbit and clock offset, which primarily showcases the performance of the space segment and
72 the ground segment. Montenbruck et al. pointed out that the SISRE could be used as a key
73 system indicator to analyze the overall performance of the ground segment and the space
74 segment^[10]. With the development of BeiDou, many scholars conducted analysis and research
75 on the SISRE of the system. Considering the data from March 2013 to September 2016, Wu
76 et al. took the precise orbit and clock offset as the standard to obtain a detailed analysis of the
77 evolution of the BDS-2 SISRE^[11]. In 2018, Montenbruck et al. employed the multi-system
78 broadcast ephemeris data to compare the SISRE of the satellite navigation systems such as
79 GPS, GLONASS, Galileo and BDS-2^[12]. And then, Ouyang et al. analyzed BDS-2 broadcast
80 navigation message from 2013 to 2018^[13]. In 2020, Yang et al. and Chen et al. respectively
81 examined the SISRE of 18 MEO satellites of the basic BDS-3 constellation, validating the
82 satisfactory performance of BDS-3 and proposing technological assumptions for future
83 developments of the system^{[14][15]}. In the same year, Montenbruck et al. studied the difference
84 in SISRE for GPS, GLONASS, Galileo, and BDS-3 (only considering BDS-3 MEO satellites)
85 ^[16], and Jiao et al. (2020). compared BDS-3 and BDS-2 broadcast ephemeris^[17]. In 2021, Xue
86 et al. mainly analyzed the influence of clock errors on BDS-3 SISRE base on the data from
87 January 1 to December 31 in the year of 2019^[18], and Chen et al. (2021) made a further
88 comparison between BDS-3 SISRE and BDS-2 SISRE^[19]. However, the existing studies on
89 SISRE for different types of satellites including MEO, GEO and IGSO after the official
90 launch of BDS-3 are insufficient, especially for the comparison between BDS-3 and other
91 systems.

92 Besides, the level of positioning accuracy, a key performance indicator for the BeiDou
93 System, has long been valued. Since the time BDS-2 began to operate, there have been plenty
94 of articles about the systemic analysis on its positioning performance^{[20][21][22][23]}. Later, with
95 the construction and development of BDS-3, multiple studies have evaluated the level of
96 positioning accuracy. With the 5 experimental BDS-3 satellites, Yang et al. and Zhang et al.
97 analyzed the observation quality of the BDS-3 new signals in terms of carrier-to-noise ratio,
98 multipath, and observed quantity combination^{[24][25]}. Zhang et al. conducted a preliminary
99 assessment about the signal quality of BDS-3 and the positioning performance of Real-Time
100 Kinematic (RTK) and Precise Point Positioning (PPP)^[26]. Shi et al. and Lv et al. considered
101 18 MEO satellites and 1 GEO satellite from the basic constellation of BDS-3 to analyze the

102 positioning performance^{[27][28]}. However, the above analyses were mostly conducted when the
103 construction of BDS-3 was incomplete. Moreover, the assessment for the full constellation
104 positioning performance of the BDS-3 new signals was limited.

105 We here present the SISRE computation method for different types of navigation
106 satellites and deduce the differential code bias (DCB) correction method for BDS-3 new
107 signals during the positioning data processing. Then the SISRE of BDS-3 is analyzed
108 including GEO, IGSO, and MEO satellites. Also, comparisons are made with BDS-2, GPS,
109 GLONASS, Galileo, and QZSS. And meanwhile, Standard Point Positioning (SPP) and PPP,
110 the two positioning modes that can best reflect the data quality of the pseudo-code and the
111 carrier phase, are adopted to perform the in-depth analysis on the positioning performance of
112 the new signals and the transitional signals for BDS-3.

113

114 **Data Processing Methods**

115 Within this section, SISRE computation method for different types of satellites is introduced,
116 which is convenient to compute and compare the SISREs of different navigation systems. To
117 evaluate performance of BDS-3 SPP and PPP, we mainly deduce the DCB correction method
118 while processing B1C or B2a signals.

119

120 **SISRE**

121 The SISRE, which involves two parts, i.e., the satellite orbit error and the satellite clock
122 offset error, is evaluated as follows. The multi-system precise orbit and clock offset are taken
123 as the standard and the broadcast ephemeris is used to derive the satellite orbit and the clock
124 offset of the corresponding epoch, analyzing their difference to gain the SISRE. During the
125 analysis, some issues should be processed, such as the antenna phase offset correction, the
126 time group delay, et al^{[12][14][16]}. Some major navigation systems such as BDS, GPS, Galileo,
127 GLONASS, and QZSS are simultaneously considered for enhanced comparison effects.

128 The computation equation of SISRE for different types of satellites is as follows:

$$129 \quad SISRE = \sqrt{(w_R \cdot R - c\delta t)^2 + w_{A,C}^2 \cdot (A^2 + C^2)} \quad (1)$$

130 where w_R and $w_{A,C}$ are corresponding weight factors that are related to the satellite altitude, as
 131 mentioned in Table 3; R , A , and C denote the radial, along-track, and normal orbit error,
 132 respectively; δt indicates the clock offset error of the satellite; and c represents the speed of
 133 light.

134

135 **Table 3** Values of weight factors for different systems. These values are mainly related to the
 136 satellite altitude.

System	w_R	$w_{A,C}^2$
BDS (MEO)	0.98	1/54
BDS (IGSO, GEO)	0.99	1/126
GPS	0.98	1/49
GLONASS	0.98	1/45
Galileo	0.98	1/61
QZSS(IGSO, GEO)	0.99	1/126

137

138 SPP and PPP processing for BDS-3

139 SPP and PPP have been elaborated extensively in the literature. The chief issue of the DCB
 140 correction is only explained here when processing the new signals of B1C and B2a for BDS-
 141 3. The reference signal of the clock offset in BeiDou broadcast ephemeris is B3I, whereas the
 142 precise clock offset products are typically calculated by the B1I and B3I ionosphere-free
 143 combination. Hence, whether the broadcast ephemeris or the precise product is in use while
 144 processing B1C or B2a, the DCB correction should be noted.

145 Here, the B1C and B2a ionosphere-free combination for PPP is taken as an example. In
 146 this case, the B1C and B2a dual-frequency pseudo-code ionosphere-free combination should
 147 be utilized as:

$$148 \quad PC_{B1C_B2a} = \rho + c(\delta t_r - \delta t_s) + \delta_{trop} + c \left(\frac{f_{B1C}^2 \tau_{B1C} - f_{B2a}^2 \tau_{B2a}}{f_{B1C}^2 - f_{B2a}^2} \right) \quad (2)$$

149 where PC_{B1C_B2a} indicates the B1C and B2a dual-frequency pseudo-code ionosphere-free
 150 combination observation; ρ indicates the geometrical distance between the receiver and the

151 satellite; c signifies the speed of light; δt_r and δt_s represent the receiver clock offset and the
 152 satellite clock offset, respectively; δ_{trop} is the tropospheric correction; f_{B1C} and f_{B2a} indicate the
 153 frequency of B1C and B2a, respectively; τ_{B1C} and τ_{B2a} denote the internal signal delay of the
 154 B1C and the B2a pseudo-code, respectively.

155 According to (2), the satellite clock offset and the internal signal delay cannot be
 156 separated. The satellite clock offset $\delta t_{st(B1C_B2a)}$ that includes the internal signal delay is
 157 defined as:

$$158 \quad \delta t_{st(B1C_B2a)} = \delta t_s - \left(f_{B1C}^2 \tau_{B1C} - f_{B2a}^2 \tau_{B2a} \right) / \left(f_{B1C}^2 - f_{B2a}^2 \right) \quad (3)$$

159 Similarly, the precise clock offset of BeiDou is often derived through the B1I and B3I
 160 ionosphere-free combination. We have

$$161 \quad \delta t_{st(B1I_B3I)} = \delta t_s - \left(f_{B1I}^2 \tau_{B1I} - f_{B3I}^2 \tau_{B3I} \right) / \left(f_{B1I}^2 - f_{B3I}^2 \right) \quad (4)$$

162 Here, $\delta t_{st(B1I_B3I)}$ signifies the satellite clock offset that contains the internal signal delay of
 163 the B1I and B3I ionosphere-free combination; f_{B1I} and f_{B3I} denote the frequency of B1I and
 164 B3I, respectively; τ_{B1I} and τ_{B3I} represent the internal signal delay of the B1I and the B3I
 165 pseudo-code, respectively; δt_s is the satellite clock offset as in (2) and (3).

166 According to (3) and (4), the relationship between $\delta t_{st(B1C_B2a)}$ and $\delta t_{st(B1I_B3I)}$ can be
 167 derived. We have

$$168 \quad \delta t_{st(B1C_B2a)} = \delta t_{st(B1I_B3I)} + \left\{ \left(f_{B1I}^2 \cdot f_{B1C}^2 \cdot (\tau_{B1I} - \tau_{B1C}) + f_{B1C}^2 \cdot f_{B3I}^2 \cdot (\tau_{B1C} - \tau_{B3I}) + \right. \right. \quad (5) \\ \left. \left. f_{B1I}^2 \cdot f_{B2a}^2 \cdot (\tau_{B2a} - \tau_{B1I}) - f_{B3I}^2 \cdot f_{B2a}^2 \cdot (\tau_{B2a} - \tau_{B3I}) \right) / \left((f_{B1I}^2 - f_{B3I}^2) \cdot (f_{B1C}^2 - f_{B2a}^2) \right) \right\}$$

169 Here, $(\tau_{B1I} - \tau_{B1C})$, $(\tau_{B1C} - \tau_{B3I})$, $(\tau_{B2a} - \tau_{B1I})$, and $(\tau_{B2a} - \tau_{B3I})$ can be derived from the DCB
 170 correction data released by the related organizations which is downloaded from
 171 <ftp://igs.ign.fr/pub/igs/products/mgex/dcb> in the following analysis. Therefore, while using
 172 the precise clock offset of BeiDou for the PPP processing of the B1C and B2a ionosphere-free
 173 combination, it is mandatory to perform the DCB correction, as represented by “{ }” in (5). In
 174 SPP processing, the similar problem need to be addressed.

175

176 **Experimental Analysis**

177 In this section, the actual measured data was analyzed after the official launching of the BDS-
178 3 service. At first, the SISRE of BDS-3 was computed and compared to that of BDS-2, GPS,
179 GLONASS, Galileo and QZSS. And then, the positioning performance of BDS-3 was
180 analyzed in both cases of SPP and PPP. In the analysis, special attention was paid to the new
181 signals of BDS-3.

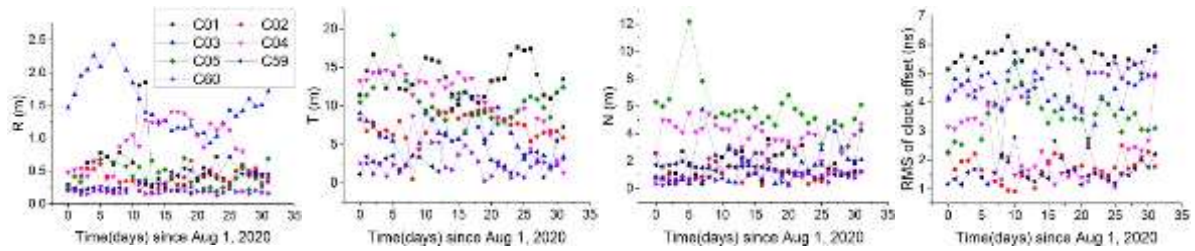
182

183 SISRE Computation

184 According to the SISRE computation method specified above, the broadcast ephemeris was
185 first used to compute the satellite position and the clock offset of 96 epochs with an interval
186 of 900s for each day. Later, considering the precise ephemeris and the precise clock offset at
187 the corresponding epoch as the standard, the errors of the orbit and the clock offset were
188 evaluated. Based on this, the SISRE was calculated. The multi-system BRDM long-filename
189 file in the RINEX format provided by Multi-GNSS Experiment (MGEX) was adopted as the
190 broadcast ephemeris. The GBM precise product was adopted as the precise orbit and the
191 precise clock offset respectively with a sampling interval of 300s and 30s.

192 The data from August 1 to September 1, 2020, a month after the official launching of the
193 BDS-3 service, were adopted. According to the three satellite categories of GEO, IGSO, and
194 MEO, the Root Mean Square (RMS) of the errors in all the epochs in a day was considered as
195 the statistical accuracy of the orbit and the clock offset. The orbit accuracy (radial, R;
196 tangential, T; normal, N) and the satellite clock offset accuracy variations were taken into
197 account for all the in-orbit operational satellites of BDS-2 and BDS-3, as illustrated in Figure
198 2, Figure 3, and Figure 4. To further compare the accuracy, the average RMSs of the R, T, or
199 N orbit error and the satellite clock offset error of each day in the counting period were
200 considered for each satellite, as highlighted in Figure 5. In Table 4, the statistical results of
201 orbit and clock offset accuracies are averaged for all the BDS-2 and BDS-3 satellites of each
202 category.

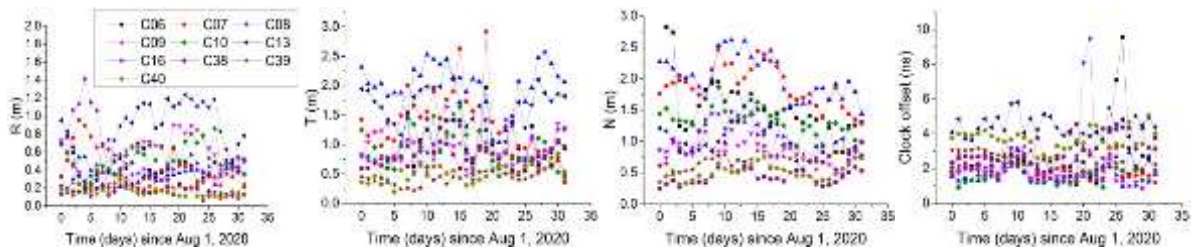
203



204

205 **Fig. 2** Orbit and clock offset accuracy variations of the GEO satellites. From left to right:
 206 Radial, tangential, normal, satellite clock offset.

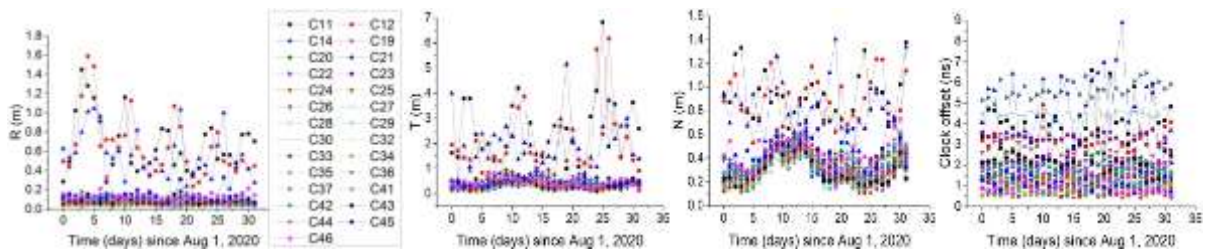
207



208

209 **Fig. 3** Orbit and clock offset accuracy variations of the IGSO satellites. From left to right:
 210 Radial, tangential, normal, satellite clock offset.

211

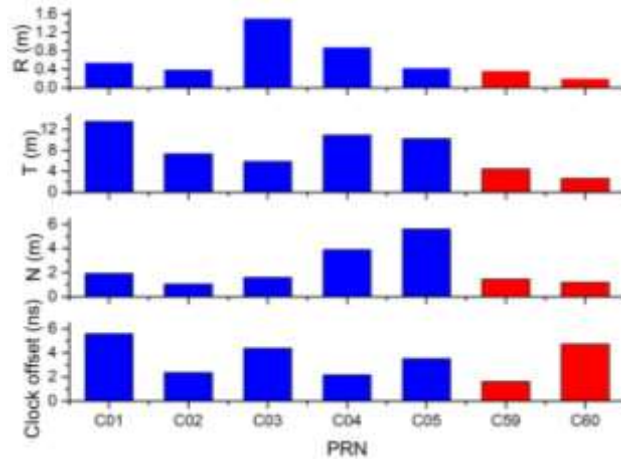


212

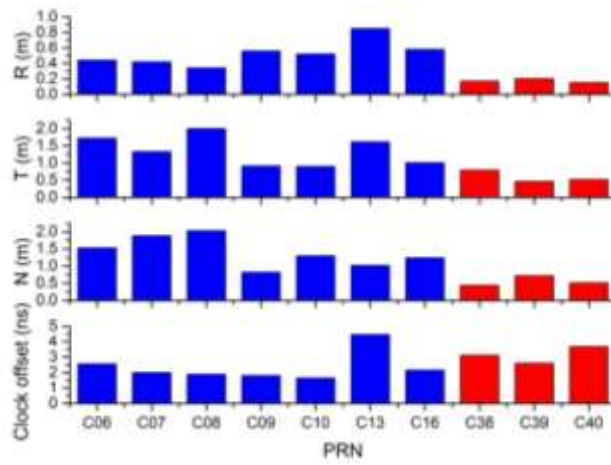
213 **Fig. 4** Orbit and clock offset accuracy variations of the MEO satellites. From left to right:
 214 Radial, tangential, normal, satellite clock offset.

215

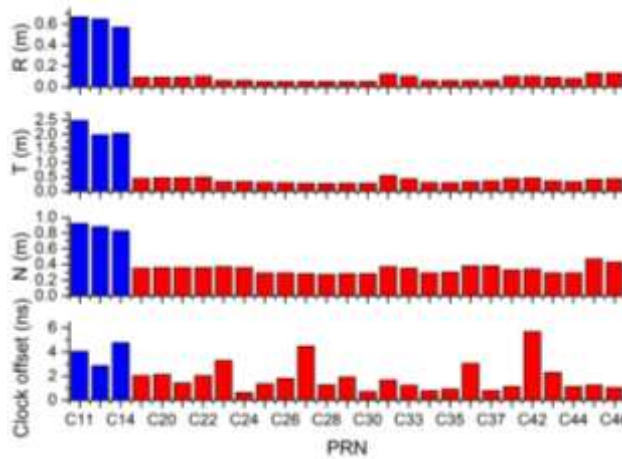
216



217



218



219 **Fig. 5** Comparison of BeiDou orbit and clock offset accuracies for three categories of GEO
220 (top), IGSO (middle), and MEO (bottom). The blue and red bars denote BDS-2 and BDS-3
221 satellites, respectively.

222

223 **Table 4** Statistics of BeiDou orbit and clock offset accuracies. The results are derived from
224 the averages of the corresponding values for all the same category of BDS-2 and BDS-3

225 satellites in Figure 5, respectively.

	GEO		IGSO		MEO	
	BDS-2	BDS-3	BDS-2	BDS-3	BDS-2	BDS-3
R(m)	0.74	0.27	0.53	0.17	0.63	0.08
T(m)	9.57	3.51	1.26	0.59	2.16	0.37
N(m)	2.81	1.32	1.37	0.56	0.88	0.34
Clock offset(ns)	3.60	3.17	2.35	3.13	3.88	1.83

226

227 The following can be seen from the above results:

228 (1) Compared to the BDS-2 GEO satellites, the BDS-3 GEO satellites of C59 and C60
229 exhibited significantly better orbit accuracies in R, T, and N directions. In terms of satellite
230 clock offset accuracy, the C59 satellite was superior to the BDS-2 satellites, while the C60
231 satellite demonstrated a relatively lower clock offset accuracy. Upon examination, it was
232 concluded that C60 was launched in March 2020 while C59 was launched in December 2018,
233 due to which the C60 satellite clock was possibly still in the process of aging and due for
234 further improvement in its performance^[29]. On average, the R-, T-, and N-direction orbit
235 accuracy and the satellite clock offset accuracy of the BDS-3 GEO satellites achieved 0.27m,
236 3.51m, 1.32m, and 3.17ns, respectively, an improvement of 63.5%, 63.3%, 53.0%, and 11.9%
237 compared to that of BDS-2.

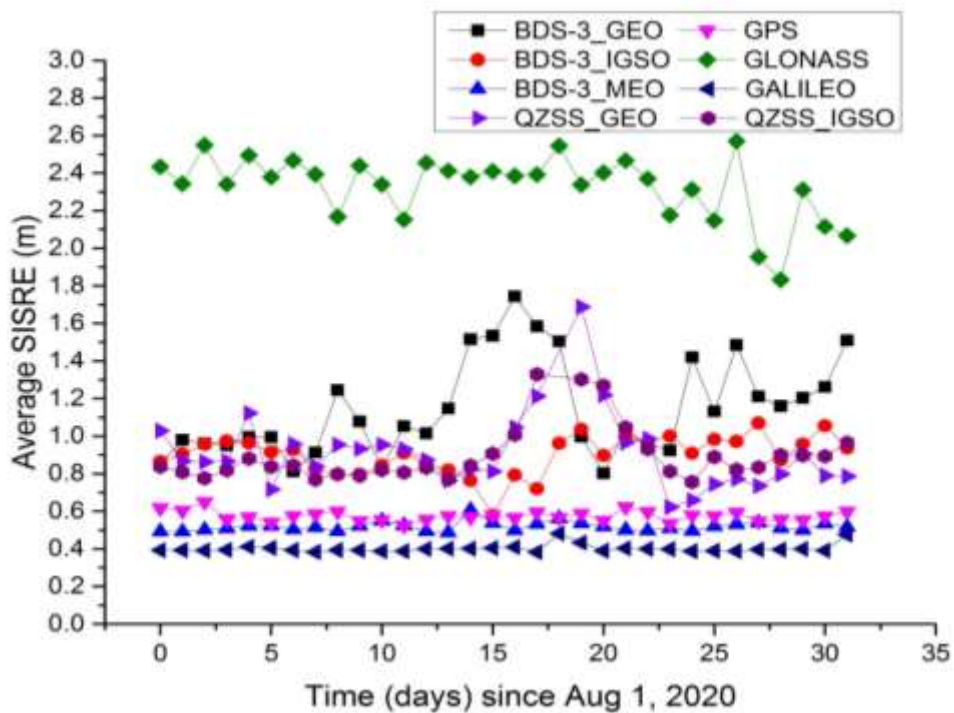
238 (2) The R-, T-, and N-direction orbit accuracy of the BDS-3 IGSO satellites were
239 remarkably higher than that of the BDS-2. However, the three IGSO satellites were all newly
240 launched in 2019, not exhibiting evident advantages in terms of the satellite clock offset
241 accuracy, similar to the case of the C60 satellite. On average, the R-, T-, and N-direction orbit
242 accuracy of the BDS-3 IGSO satellites were 0.17m, 0.59m, and 0.56m, respectively, which
243 was improved by 67.9%, 53.1%, and 59.1%, respectively, compared to that of the BDS-2. The
244 satellite clock offset accuracy reached 3.13ns, which was marginally inferior to that of the
245 BDS-2 IGSO satellites.

246 (3) The BDS-3 MEO satellites displayed higher R-, T-, N-direction orbit accuracies than
247 the BDS-2. They also delivered a comparatively steady and sound performance in terms of
248 the satellite clock offset accuracy, except for a few of them (e.g., the C42 satellite launched in
249 December 2019). On average, the R-, T-, and N-direction orbit accuracy and the satellite

250 clock offset accuracy of BDS-3 MEO satellites were 0.08m, 0.37m, 0.34m, and 1.83ns,
251 respectively, illustrating a significant improvement of 87.3%, 82.9%, 61.4%, and 52.8%,
252 respectively, compared to that of BDS-2.

253 To further compare the SISRE between BDS-3 and other systems, the analysis data above
254 were also used. Initially, the SISRE of each epoch for every BDS-3 satellite was calculated.
255 Then, the satellites were grouped into the three categories of GEO, IGSO, and MEO, and had
256 the SISRE averaged in each group for all the epochs of each day. Besides, the same accuracy
257 statistics were run for the SISRE of GPS, GLONASS, Galileo, and QZSS, to perform a better
258 comparison. Moreover, QZSS included 1 GEO satellite and 3 IGSO satellites at the time,
259 which were counted separately as in the case of BDS-3. As for the other systems, only MEO
260 satellites were involved, thus demanding no categorization. Figure 6 illustrates the daily
261 statistical result of SISRE during the analysis period for each system, while Table 5 enlists the
262 average.

263



264

265 **Fig. 6** SISREs of major systems from Aug 1, 2020 to Sep 1, 2020. For comparison, BDS-3
266 satellites were grouped into the three categories of GEO, IGSO, and MEO. QZSS satellites
267 are also made a similar classification.

268

269 **Table 5** Average SISRE for major systems. The results of different systems are the average of
270 the SISREs for all days from Aug 1, 2020 to Sep 1, 2020.

System	SISRE(m)
BDS-3_GEO	1.15
BDS-3_IGSO	0.90
BDS-3_MEO	0.52
GPS	0.57
GLONASS	2.33
Galileo	0.40
QZSS_GEO	0.91
QZSS_IGSO	0.90

271

272 The following can be obtained from the results highlighted in Figure 6 and Table 5:

273 (1) The BDS-3 GEO, IGSO, and MEO satellites displayed an average SISRE of 1.15
274 m, 0.90 m, and 0.52 m, respectively.

275 (2) Among the four primary global satellite navigation systems, when only the MEO
276 satellites were considered, Galileo introduced the best space signal accuracy with an average
277 SISRE of 0.40 m. Following Galileo, BDS-3 and GPS showcased an average SISRE of 0.52
278 m and 0.57 m, respectively. GLONASS demonstrated the worst performance with an average
279 SISRE of merely 2.33 m.

280 (3) The BDS-3 IGSO satellites, as well as the QZSS IGSO satellites, had an average
281 SISRE of 0.90m. However, the average SISRE of the QZSS GEO satellites reached 0.91m,
282 which was slightly better than the value of 1.15 m for the BDS-3 GEO satellites. Considering
283 that the BDS-3 C60 satellite was still new since its launch and has room for improvement in
284 its satellite clock offset accuracy, this situation can be treated as normal. In the future, the
285 accuracy may be further enhanced with the progressive service provided by the C61 satellite.

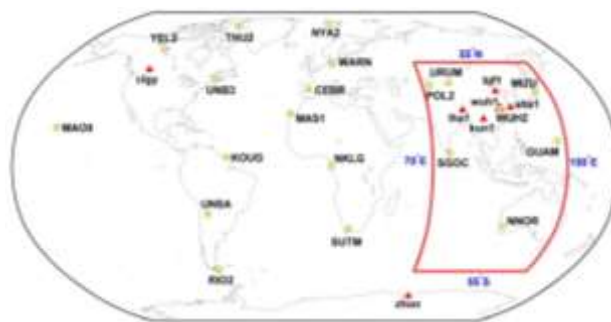
286

287 Analysis of Positioning Accuracy

288 To enhance the presentation of the analysis result of the positioning accuracy, when selecting
289 the analysis data, the spatial and temporal coverage was fully considered. In terms of spatial

290 coverage, 27 multi-system observation stations distributed globally were chosen, as
291 demonstrated in Figure 7. Among them, 20 MGEX observation stations and 7 iGMAS
292 (international GNSS monitoring and assessment service) observation stations were included,
293 respectively labeled as ‘■’ and ‘▲’. For convenient comparison, a red box is drawn in Figure
294 7 that highlights the key BDS service area (55°S—55°N, 70°E—150°E). Moreover, to
295 improve the temporal coverage of the analysis, from the days after the official service launch
296 of the system, the observation data were chosen on the 1st date of August, September,
297 October, November, and December in the year 2020, and on January 1, 2021, with a sampling
298 interval of 30 s. Later, BDS-3 SPP and PPP processing were conducted for the data collected
299 on these six days. The results were further compared with the known coordinates to evaluate
300 the positioning accuracy.

301



302

303 **Fig. 7** Distribution map of the observation stations. A red box is drawn to highlight the key
304 BDS service area (55°S—55°N, 70°E—150°E). The MGEX station names are in the capital
305 letters and the iGMAS station names are in the lowercase letters, which are also respectively
306 labeled as ‘■’ and ‘▲’.

307

308 *SPP Accuracy*

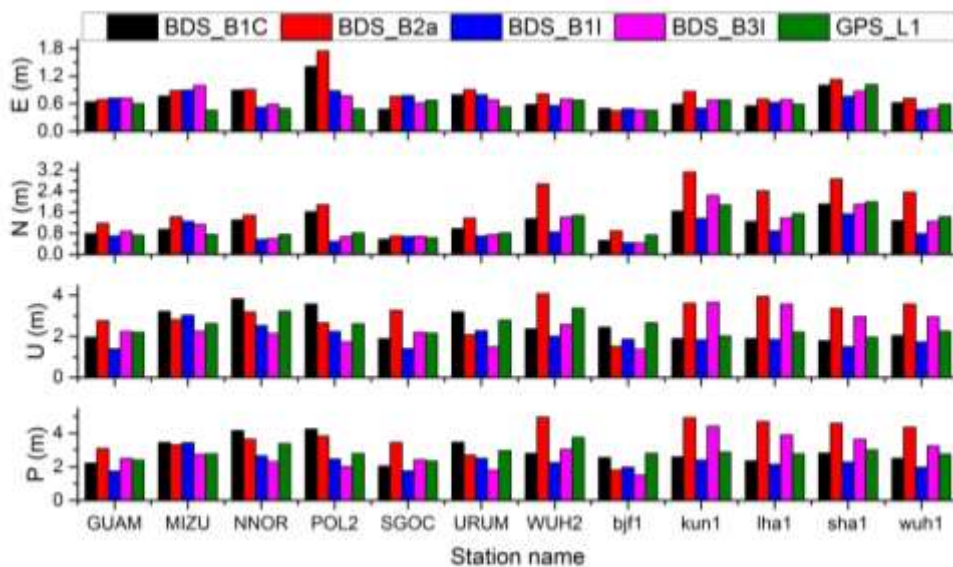
309 This section mainly analyzes SPP accuracy of BDS-3 in the two cases of single-frequency
310 SPP and double-frequency SPP. In the former case, the single-frequency signals including
311 B1C, B2a, B1I and B3I will be considered, and in the latter case, the double-frequency signals
312 including B1C+B2a and B1I+B3I will be focused on.

313

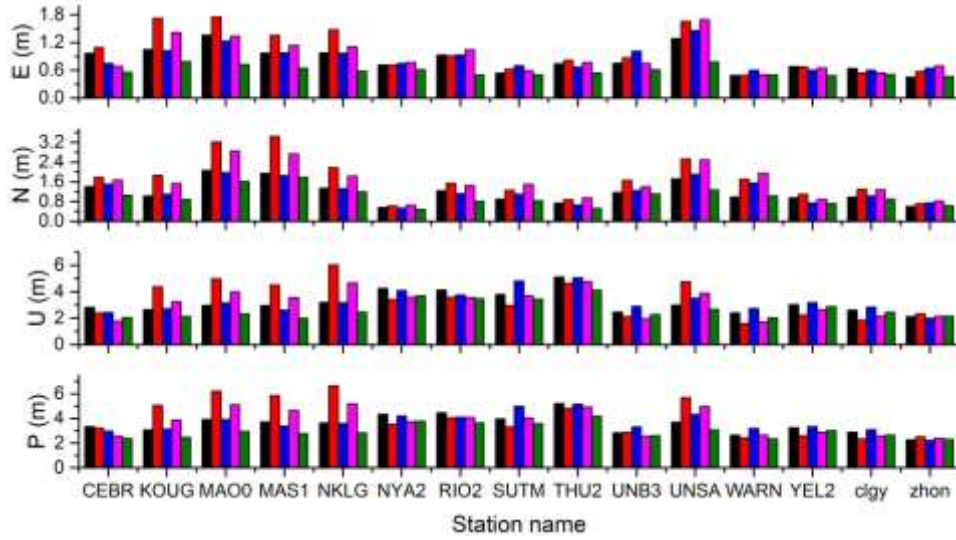
314 (1) Single-frequency SPP

315 The open positioning and navigation service signals of BDS-3 comprise the new signals of
 316 B1C and B2a along with the transitional signals of B1I and B3I. The former is only broadcast
 317 by the BDS-3 MEO and IGSO satellites, whereas the latter is broadcast by all the satellites of
 318 BDS-3 and BDS-2 category, as mentioned in Table 2. To assess the positioning performance
 319 of the signals, the observed pseudo-code for each single-frequency signal was utilized for SPP
 320 in each epoch. The RMSs of the east (E), north (N), up (U), and three-dimensional positioning
 321 errors for each epoch were also counted. For better comparison, the single-frequency
 322 positioning of the GPS L1 C/A code is also displayed in Figure 8. Considering this, the
 323 positioning error RMS of each direction was averaged for all the observation stations, the
 324 results for which are enlisted in Table 6. It must be noted that single-frequency SPP has a
 325 wide range of application situations, the accuracy of which constitutes a key performance
 326 factor in the system construction.

327



328



329
 330 **Fig. 8** RMS statistics of single-frequency SPP positioning errors for stations in the Asian-
 331 Pacific region (top) and other regions (bottom). The MGEX station names are in the capital
 332 letters and the iGMAS station names are in the lowercase letters.

333

334 **Table 6** Average of the positioning errors RMS over all observation stations for single-
 335 frequency SPP (unit: m)

Signal	E		N		U		P	
	Asia- Pacific region	Other region	Asia- Pacific region	Other region	Asia- Pacific region	Other region	Asia- Pacific region	Other region
	BDS_B1C	0.73	0.84	1.18	1.17	2.51	3.16	2.93
BDS_B2a	0.89	1.02	1.86	1.72	3.07	3.45	3.78	4.08
BDS_B1I	0.66	0.86	0.85	1.22	1.97	3.26	2.30	3.66
BDS_B3I	0.69	0.91	1.11	1.60	2.43	3.15	2.80	3.74
GPS_L1	0.60	0.59	1.12	0.99	2.51	2.67	2.88	2.97

336

337 The following can be concluded from Figure 8 and Table 6:

338 (1) Whether it was the Asian-Pacific region or other regions, the three-dimensional
 339 accuracy of single-frequency SPP for each signal frequency of BeiDou has always been better
 340 than 5 m on the whole. The east or north positioning result was particularly superior to that of
 341 the up direction. For all the four frequencies of BeiDou, the positioning accuracy was higher

342 in the Asian-Pacific region than in other regions, since more satellites were visible in Asia-
343 Pacific region because of the special BDS constellation.

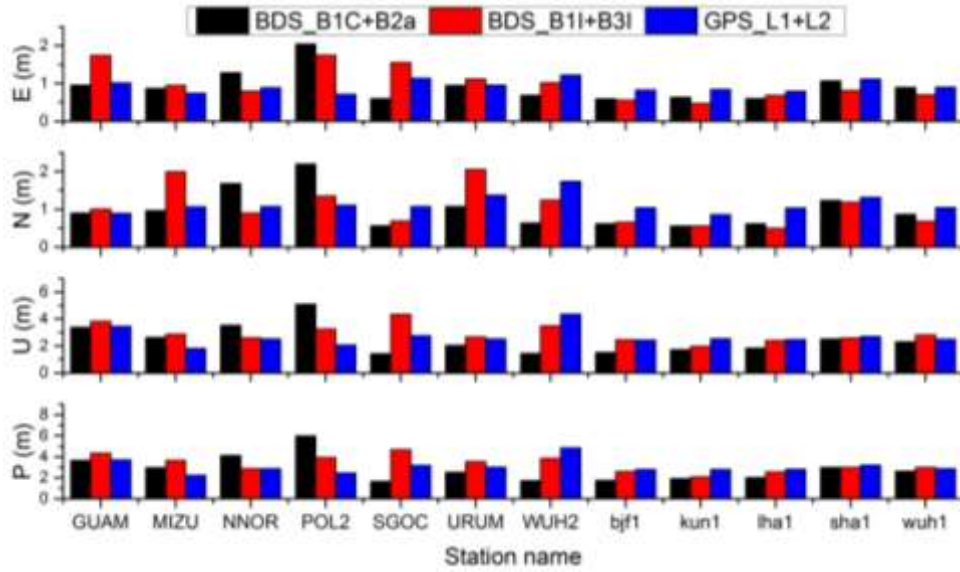
344 (2) Compared to the GPS L1 C/A code, the BDS-3 B1C, B2a, B1I, and B3I signals
345 could achieve a comparable single-frequency SPP result. In the Asian-Pacific region, the
346 three-dimensional positioning accuracies of B1I and B3I were comparatively better, achieving
347 2.30 m and 2.80 m, respectively, which were better than 2.88 m of GPS. In other regions, the
348 three-dimensional positioning accuracy of B1C was found to be 3.55 m, which was the best
349 among the four BeiDou signals, though marginally worse than 2.97 m of GPS. The causes for
350 the phenomena above are as follows. B1I and B3I are transitional signals that are broadcast by
351 both BDS-2 and BDS-3, which have an obvious advantage in the number of visible satellites
352 in the Asian-Pacific region, thereby delivering higher positioning accuracy over there. In
353 other regions, with only 3 BDS-2 MEO satellites, B1I and B3I do not possess a superior
354 number of visible satellites. On the other hand, as a newly designed signal and being
355 compatible with GPS L1 and Galileo E5, B1C possesses a significant advantage in the
356 performance of capturing and tracking. However, it is the 24 BDS-3 MEO satellites that
357 broadcast the B1C signal in other regions, which are still exceptionally fewer than the 31 in-
358 orbit functioning satellites of GPS^[30]. This is also the chief reason for its positioning accuracy
359 being slightly lower than that of GPS.

360

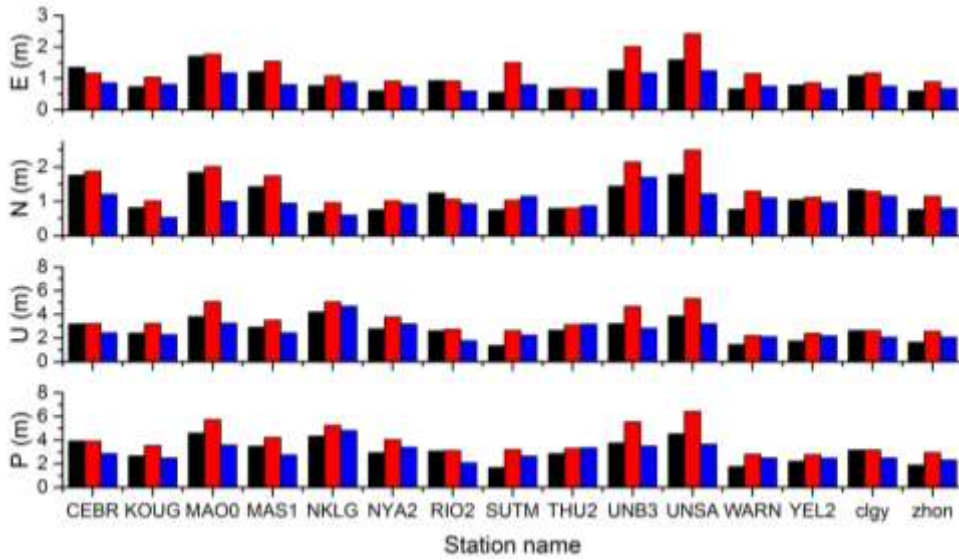
361 (2) Dual-frequency SPP

362 Here, dual-frequency SPP processing was executed for the two dual-frequency pseudo-code
363 combinations, namely B1C+B2a and B1I+B3I. The output was compared with the L1+L2
364 dual-frequency pseudo-code SPP result of GPS. The statistical approach for the accuracy was
365 the same as that of the single-frequency SPP, and the results are demonstrated in Figure 9 and
366 Table 7.

367



368



369

370 **Fig. 9** RMS statistics of dual-frequency SPP positioning errors for stations in the Asian-
 371 Pacific region (top) and other regions (bottom). The MGEX station names are in the capital
 372 letters and the iGMAS station names are in the lowercase letters.

373

374 **Table 7** Average of positioning errors RMS over all observation stations for dual-frequency
 375 SPP (unit: m)

Signal	E		N		U		P	
	Asia- Pacific region	Other region	Asia- Pacific region	Other region	Asia- Pacific region	Other region	Asia- Pacific region	Other region
	BDS-3_B1C+B2a	0.80	0.80	0.82	0.99	2.09	2.27	2.39

BDS-3_B1I+B3I	0.69	0.73	0.76	1.15	2.48	2.90	2.70	3.34
GPS_L1+L2	0.85	0.73	1.00	0.95	2.51	2.37	2.83	2.67

376

377 The following can be observed from Figure 9 and Table 7.

378 (1) BeiDou B1C+B2a and B1I+B3I, the two dual-frequency SPP schemes, exhibited
 379 relatively high accuracy in the Asian-Pacific region. Moreover, whether in Asia-Pacific or
 380 other regions, B1C+B2a dual-frequency positioning was significantly superior to B1I+B3I.
 381 Although more satellites broadcast B1I and B3I signals in Asia-Pacific, the more the distance
 382 between the two frequencies in dual-frequency positioning, the better the correction of
 383 ionospheric delay after their combination. In this regard, B1C+B2a is more advantageous
 384 since its positioning result was still better than that of B1I+B3I, even with fewer satellites.

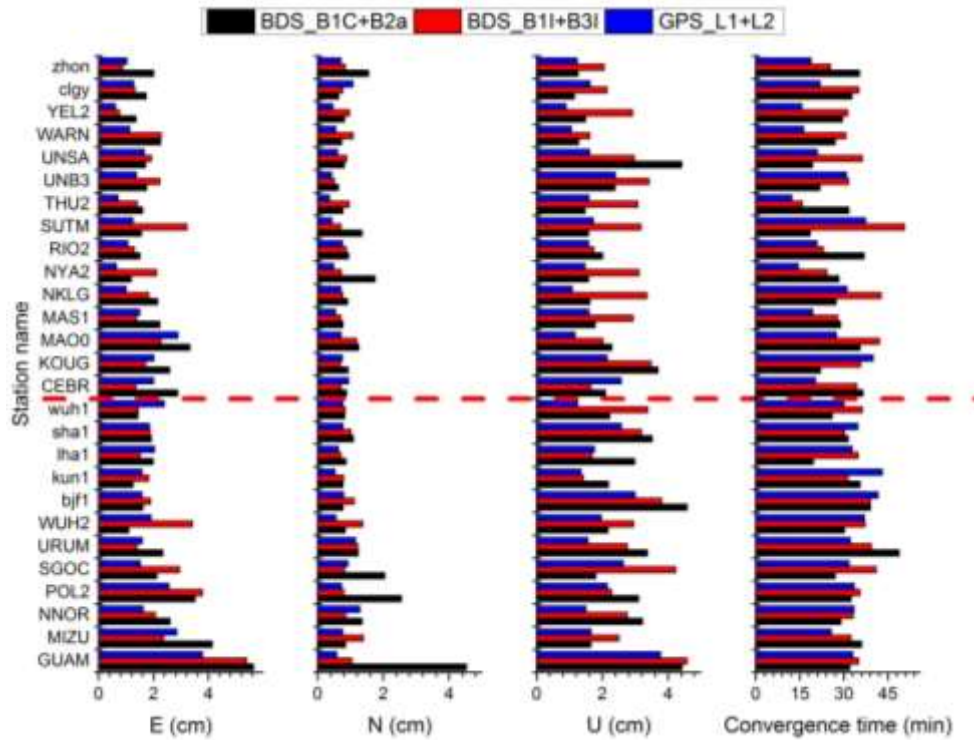
385 (2) In the Asian-Pacific region, the three-dimensional accuracy of BeiDou B1C+B2a
 386 dual-frequency SPP reached 2.39 m, marginally better than 2.83 m of GPS L1+L2. In other
 387 regions, the three-dimensional accuracy of BeiDou B1C+B2a dual-frequency SPP reached
 388 2.63 m, slightly better than 2.67 m of GPS L1+L2. Considering the accuracy of the pseudo-
 389 code, it could be deemed that the two were fundamentally equal.

390

391 *PPP Accuracy*

392 The two dual-frequency pseudo-code and carrier phase combinations of B1C+B2a and
 393 B1I+B3I were adopted here. Utilizing the same observation data from the stations in the
 394 Figure 7, the PPP experiment for BeiDou was conducted, followed by computing the
 395 positioning accuracy after convergence. For convenient comparison, GPS L1+L2 dual-
 396 frequency PPP was conducted at the same time. The convergence standard was set as when
 397 the E-, N-, and U-direction deviations were all lesser than 10 cm for more than 20 epochs^[31].
 398 The PPP convergence time was also computed for each processing mode. The above results
 399 are mentioned in Figure 10. The results below the red dash line are from the Asian-Pacific
 400 observation stations, while the ones above are from the stations in other regions.

401



402

403 **Fig. 10** RMS statistics of dual-frequency PPP positioning errors and convergence time for
 404 stations in the Asian-Pacific region (below the red dash line) and other regions (above the red
 405 dash line). The MGEX station names are in the capital letters and the iGMAS station names
 406 are in the lowercase letters.

407

408 **Table 8** Average of positioning errors RMS and convergence time over all observation
 409 stations for PPP

Signal	E(cm)	N(cm)	U(cm)	Convergence time (min)
BDS3-3_B1C+B2a	2.2	1.2	2.4	30.3
BDS-3_B1I+B3I	2.1	0.9	2.7	33.8
GPS_L1+L2	1.7	0.7	1.8	28.0

410

411 According to the comparison of the results in Figure 9, both the new signal of B1C+B2a
 412 and the transitional signal of B1I+B3I could provide PPP results with centimeter accuracy to
 413 the observation stations globally. The Asian-Pacific region, though with a larger number of
 414 visible satellites, did not exhibit any obvious advantage. This is because the more visible
 415 satellites included some GEO satellites that had marginally lower precise orbit and clock

416 offset accuracies, failing to improve the PPP accuracy significantly^[32]. Hence, the observation
417 stations here were not divided according to their location but considered altogether. The
418 RMSs of E-, N-, and U-direction positioning errors were counted for all the observation
419 stations in different positioning modes, as mentioned in Table 8. The following can be
420 inferred from the above results.

421 (1) After the convergence of B1C+B2a, the E-, N-, and U-direction accuracies achieved
422 2.2 cm, 1.2 cm, and 2.4 cm, respectively, on par with the processing results of B1I+B3I;
423 though slightly worse than that of GPS L1+L2. The accuracy of BeiDou PPP could be further
424 improved due to the evolution of future precise products.

425 (2) Except for a few observation stations, the PPP convergence time for BDS-3
426 B1C+B2a or B1I+B3I was fundamentally equal to that of the GPS L1+L2, being
427 approximately 30 minutes.

428

429 **Conclusions**

430 In the present study, the SISRE computation method for different types of navigation
431 satellites was present and the DCB correction method for BDS-3 new signals was deduced.
432 In-depth analysis of the service accuracy levels have been analyzed from the perspective of
433 BDS-3 SISRE and SPP or PPP positioning performance, leading to the following conclusions:

434 (1) Compared to the BDS-2 satellites, the BDS-3 MEO, IGSO and GEO satellites
435 exhibited significantly improved R, T, and N orbit accuracies. Except for a couple of newly
436 launched satellites, the satellite clock offset accuracy was also remarkably enhanced.

437 (2) The average SISREs of the BDS-3 MEO IGSO, and GEO satellites were 0.52m
438 0.90m and 1.15m, respectively. Compared to the four major global satellite navigation
439 systems consisting of MEO satellites, the SISRE of the BDS-3 MEO satellites was slightly
440 inferior to 0.4 m of Galileo, slightly superior to 0.57 m of GPS, and remarkably superior to
441 2.33 m of GLONASS. The SISRE of BDS-3 IGSO was on par with 0.90 m of QZSS IGSO.
442 However, as the BDS-3 GEO satellites were newly launched and not completely functioning
443 in orbit, their average SISRE was marginally worse than 0.91 m of the QZSS GEO satellites.

444 (3) Single-frequency SPP of BDS-3 B1C, B2a, B1I, and B3I could all achieve
445 remarkable positioning accuracy, with an overall three-dimensional positioning accuracy level

446 better than 5 m. Among them, the B1I signal delivered the best positioning accuracy in the
447 Asian-Pacific region while the B1C was leading in the other regions. Owing to the advantage
448 in signal frequency, the dual-frequency SPP of B1C+B2a expressed better positioning
449 accuracy compared to the transitional signal of B1I+B3I. The three-dimensional positioning
450 accuracy levels for B1C+B2a of 2.39 m and 2.63 m were achieved respectively in the Asian-
451 Pacific region and the other regions. Since there were more visible satellites in the Asia-
452 Pacific, the positioning accuracy of BDS-3 was marginally better than that of GPS.

453 (4) After convergence, the PPP accuracy of BDS-3 B1C+B2a or B1I+B3I was on the
454 level of centimeters, slightly inferior to that of GPS L1+L2. The convergence time, however,
455 was similar for all three, which was approximately 30 minutes.

456

457 **Acknowledgment** This study was supported by the National Natural Science Foundation of
458 China (Grant No. 41804035). Many thanks to the IGS MGEX, iGMAS and GFZ for
459 providing the experimental data.

460

461 **Data Availability**

462 All data generated or analyzed during this study are included in this published article.

463

464 **References**

465 [1] CSNO. Development of the BeiDou Navigation Satellite System (Version 4.0). Accessed
466 December 2019.

467 [2] Yang Y, Gao W, Guo S, Mao Y, Yang Y. Introduction to BeiDou-3 navigation satellite
468 system. *Navigation*. 66(1), 7-18. <https://doi.org/10.1002/navi.291> (2019).

469 [3] CSNO. BeiDou navigation satellite system signal in space interface control document
470 open service signal B1C (version 1.0). Accessed December 2017.

471 [4] CSNO. BeiDou navigation satellite system signal in space interface control document
472 open service signal B2a (version 1.0). Accessed December 2017.

473 [5] Lu M, Li W, Yao Z, Cui X. Overview of BDS III new signals. *Navigation*. 66(1), 19-35.

-
- 474 <https://doi.org/10.1002/navi.296> (2019).
- 475 [6] CSNO. BeiDou navigation satellite system signal in space interface control document
476 open service signal B1I (version 3.0). Accessed February 2019.
- 477 [7] CSNO. BeiDou navigation satellite system signal in space interface control document
478 open service signal B3I (version 1.0) . Accessed February 2018.
- 479 [8] Liu L, Zhang T, Zhou S, Hu X, Liu X. Improved design of control segment in BDS-3.
480 Navigation. 66(1), 37-47. <https://doi.org/10.1002/navi.297> (2019).
- 481 [9] Yang Y et al. Inter-satellite link enhanced orbit determination for BeiDou-3. The Journal
482 of Navigation. 73(1), 115-130. <https://doi.org/10.1017/S0373463319000523> (2020).
- 483 [10] Montenbruck O, Steigenberger P, Hauschild A. Broadcast versus precise ephemerides: a
484 multi-GNSS perspective. GPS Solutions. 19(2), 321-333. [https://doi.org/10.1007/s10291-](https://doi.org/10.1007/s10291-014-0390-8)
485 [014-0390-8](https://doi.org/10.1007/s10291-014-0390-8) (2015).
- 486 [11] Wu Y, Liu X, Liu W, Ren J, Lou Y, Dai X, Fang X. Long-term behavior and statistical
487 characterization of BeiDou signal-in-space errors. GPS Solut. 21(24), 1907-1922.
488 <https://doi.org/10.1007/s10291-017-0663-0> (2017).
- 489 [12] Montenbruck O, Steigenberger P, Hauschild A. Multi-GNSS signal-in-space range error
490 assessment–Methodology and results. Adv Space Res. 61(12), 3020-3038.
491 <https://doi.org/10.1016/j.asr.2018.03.041> (2018).
- 492 [13] Ouyang C, Shi J, Shen Y, Li L. Six-Year BDS-2 Broadcast Navigation Message Analysis
493 from 2013 to 2018: Availability, Anomaly, and SIS UREs Assessment. Sensors. 19(12),
494 2767. <https://doi.org/10.3390/s19122767> (2019).
- 495 [14] Yang Y, Mao Y, Sun B. Basic performance and future developments of BeiDou global
496 navigation satellite system. Satellite Navigation. 1(1),1-8. [https://doi.org/10.1186/s43020-](https://doi.org/10.1186/s43020-019-0006-0)
497 [019-0006-0](https://doi.org/10.1186/s43020-019-0006-0) (2020).
- 498 [15] Chen J et al. SIS accuracy and service performance of the BDS-3 basic system. Sci.
499 China-Phys. Mech. Astron. 63(6), 269511. <https://doi.org/10.1007/s11433-019-1468-9>
500 (2020).
- 501 [16] Montenbruck O, Steigenberger P, Hauschild A. Comparing the ‘Big 4’-A User's View on

-
- 502 GNSS Performance. In: 2020 IEEE/ION Position, Location and Navigation Symposium
503 (PLANS), IEEE, pp 407-418 (2020).
- 504 [17]Jiao G , Song S , Liu Y , Su K, Cheng N, Wang S. Analysis and Assessment of BDS-2
505 and BDS-3 Broadcast Ephemeris: Accuracy, the Datum of Broadcast Clocks and Its
506 Impact on Single Point Positioning. Remote Sensing. 12(13), 2081.
507 <https://doi.org/10.3390/rs12132081> (2020).
- 508 [18]Xue B , Wang H , Yuan Y. Performance of BeiDou-3 signal-in-space ranging errors:
509 accuracy and distribution. GPS Solut. 25(1), 23. [https://doi.org/10.1007/s10291-020-](https://doi.org/10.1007/s10291-020-01057-z)
510 [01057-z](https://doi.org/10.1007/s10291-020-01057-z) (2021).
- 511 [19]Chen G , Zhou R , Hu Z , Lv Y, Zhao Q. Statistical characterization of the signal-in-space
512 errors of the BDS: a comparison between BDS-2 and BDS-3. GPS Solut. 25(3), 112.
513 <https://doi.org/10.1007/s10291-021-01150-x> (2021).
- 514 [20]He H, Li J, Yang Y, Xu J, Guo H, Wang A. Performance assessment of single- and dual-
515 frequency BeiDou/GPS single-epoch kinematic positioning. GPS Solut. 18(3), 393-403.
516 <https://doi.org/10.1007/s10291-013-0339-3> (2014).
- 517 [21]Montenbruck O, Hauschild A, Steigenberger P, Hugentobler U, Teunissen P, Nakamura
518 S. Initial assessment of the COMPASS/BeiDou-2 regional navigation satellite system.
519 GPS Solut. 17(2), 211-222. <https://doi.org/10.1007/s10291-012-0272-x> (2013).
- 520 [22]Shi C, Zhao Q, Hu Z, Liu J. Precise relative positioning using real tracking data from
521 COMPASS GEO and IGSO satellites. GPS Solut. 17(1), 103-119.
522 <https://doi.org/10.1007/s10291-012-0264-x> (2013).
- 523 [23]Yang Y et al. Preliminary assessment of the navigation and positioning performance of
524 BeiDou regional navigation satellite system. Sci China Earth Sci. 57(1), 144-152.
525 <https://doi.org/10.1007/s11430-013-4769-0> (2014).
- 526 [24]Yang Y, Xu Y, Li J, Yang C. Progress and performance evaluation of BeiDou global
527 navigation satellite system: Data analysis based on BDS-3 demonstration system. Sci
528 China Earth Sci. 61(5), 614-624. <https://doi.org/10.1007/s11430-017-9186-9> (2018).
- 529 [25]Zhang X, Wu M, Liu W, Li X, Yu S, Lu C, Wickert J. Initial assessment of the
530 COMPASS/BeiDou-3: new-generation navigation signals. J Geod. 91(10), 1225-1240.
531 <https://doi.org/10.1007/s00190-017-1020-3> (2017).

-
- 532 [26]Zhang Z, Li B, Nie L, Wei C, Jia S, Jiang S. Initial assessment of BeiDou-3 global
533 navigation satellite system: signal quality, RTK and PPP. *GPS Solut.* 23(4), 111.
534 <https://doi.org/10.1007/s10291-019-0905-4> (2019).
- 535 [27]Shi J, Ouyang C, Huang Y, Peng W. Assessment of BDS-3 global positioning service:
536 ephemeris, SPP, PPP, RTK, and new signal. *GPS Solut.* 24(3), 81.
537 <https://doi.org/10.1007/s10291-020-00995-y> (2020)
- 538 [28]Lv Y, Geng T, Zhao Q, Xie X, Zhou R. Initial assessment of BDS-3 preliminary system
539 signal-in-space range error. *GPS Solut.* 24(1), 16. [https://doi.org/10.1007/s10291-019-](https://doi.org/10.1007/s10291-019-0928-x)
540 [0928-x](https://doi.org/10.1007/s10291-019-0928-x) (2019).
- 541 [29]Guo S , Cai H, Meng Y, Geng C, Jia X, Mao Y, Geng T, Rao Y, Zhang H, Xie X. BDS-3
542 RNSS technical characteristics and service performance. *Acta Geodaetica et*
543 *Cartographica Sinica.* 48(7), 810-821. <https://doi.org/10.11947/j.AGCS.2019.20190091>
544 (2019).
- 545 [30]GPS official website. Space Segment. <https://www.gps.gov/systems/gps/space/> (2021).
- 546 [31]Zhang X, Li P, Guo F. Ambiguity resolution in precise point positioning with hourly data
547 for global single receiver. *Adv Space Res.* 51(1), 153-161.
548 <https://doi.org/10.1016/j.asr.2012.08.008> (2013).
- 549 [32]Zhao Q, Guo J, Li M, Qu L, Hu Z, Shi C, Liu J. Initial results of precise orbit and clock
550 determination for COMPASS navigation satellite system. *J Geod.* 87(5), 475-486.
551 <https://doi.org/10.1007/s00190-013-0622-7> (2013).

552

553 **Author Biographies**

554 **Weiping Liu** obtained his Ph.D. degree from and is now an associate professor at
555 Information Engineering University. His current research mainly concentrates on precise
556 orbit determination and positioning of GNSS.

557 **Bo Jiao** is a lecturer at Information Engineering University. He obtained his Bachelor's
558 degree and Master's degree both from Information Engineering University. His research
559 mainly focuses on precise point position ambiguity resolution.

560 **Jinming Hao** is a professor at Information Engineering University. His research interests

561 include GNSS monitoring and evaluation, precise orbit determination and mathematical
562 geodesy.

563 **Zhiwei Lv** obtained his Ph.D. degree from and is now is a professor at Information
564 Engineering University. His current research focuses on performance evaluation of BDS
565 satellite navigation system.

566 **Jiantao Xie** obtained his Ph.D. degree from and is now a lecturer at Information Engineering
567 University. His research interests include GNSS precise positioning and BDS application.

568 **Jing Liu** is now a Ph.D. student at Information Engineering University. Her research mainly
569 focuses on combined data processing of LEO- and ground-based GNSS observations.